Zero voltage switching driver and flyback transformer for generation of atmospheric pressure plasma jet

Cite as: AIP Conference Proceedings **1883**, 020023 (2017); https://doi.org/10.1063/1.5002041
Published Online: 14 September 2017

Rosnah Mohd Zin, Chin Fhong Soon, Mohd Zuhri Ab Sani, Elfa Rizan Rizon, Kian Sek Tee, Mohd Khairul Ahmad, Nabihah@Nornabihah Ahmad, Warsuzarina Mat Jubadi, and Nafarizal Nayan

Zero Voltage Switching Driver and Flyback Transformer for Generation of Atmospheric Pressure Plasma Jet

Rosnah Mohd Zin[1], Chin Fhong Soon [1,2,a)], , Mohd Zuhri Ab Sani[1], Elfa Rizan Rizon[1], Kian Sek Tee[1], Mohd Khairul Ahmad [1,2], Nabihah@Nornabihah Ahmad[1], Warsuzarina Mat Jubadi[1], Nafarizal Nayan[1, 2b)]

[1]*Faculty of Electrical and Electronic Engineering, Universiti Tun Hussein Onn Malaysia, 86400 Parit Raja, Batu Pahat, Johor, Malaysia.*
[2]*Biosensor and Bioengineering Laboratory, MiNT-SRC, Universiti Tun Hussein Onn Malaysia, 86400 Parit Raja, Batu Pahat, Johor, Malaysia.*

[a)]Corresponding author: soon@uthm.edu.my
[b)]nafarizal@uthm.edu.my

Abstract. There are increasing interests in the application of cold atmospheric plasma device for the application in surface science and medical field. Numerous studies focused on the effects of plasma emission onto living organisms. This report presents the application of a power driver circuit for induction of cold atmospheric plasma (CAP). The system consists of a resonant inverter of Zero Voltage Switching (ZVS) circuit powered by a 12Vdc input voltage which is coupled to a flyback transformer in generation of high voltage up to 24.5 kV. The output voltage from the ZVS driver and flyback transformer to the plasma torch (quartz tube) was determined using Falstad circuit simulation. The simulation on the waveforms generated from the ZVS circuit correlated well with the actual voltage measurement at the output of the ZVS circuit. The peak voltage dropped across a parallel capacitor coupled to the flyback transformer is approximately 36 V. The atmospheric pressure plasma jet (APPJ) purged with Argon gas at a flow rate of 50 l/min was exposed to a leaf for 5 seconds. This created pin holes in the exposed area of the leaf indicating high temperature was induced at the focused spot of the plasma. An atmospheric pressure plasma jet (APPJ) system has been developed for with potential application in destructive medicine.

INTRODUCTION

Plasma is one of the four fundamentals states of matter other than solid, liquid and gas. The structural form of plasma are filaments, beams and double layers of beams because of the influence of the electromagnetic field [1]. This is because plasma doesn't have a definitive shape and volume unless it is enclosed in a container [2, 3]. Cold atmospheric plasma (CAP) is different from the enclosed plasma because of the generated plasma is generated and released at the atmospheric pressure [4]. Atmospheric pressure plasma jet (APPJ), dielectric barrier discharged (DBD), plasma needle and plasma pencil are among the methods used for producing CAP [4]. Due to the ability of CAP to operate at atmospheric pressure, CAP is applied widely in biomedical engineering to prevent formation of biofilm, inhibit the growth of microbes, tooth whitening, dental instrument sterilization, inducing cell death and biochip fabrication [4-6]. High energy is needed to generate plasma. In the configuration of generating plasma with APPJ, a pair of high voltage positive (anode) and ground (cathode) electrodes are attached to a quartz tube or plasma torch. The anode can be inserted in the cylinder of the quartz tube and the anode can be attached to the quartz tube [6] or being a base off the tube. Different type of carrier gases such as helium, nitrogen, argon, oxygen and air can be infused through the quartz tube [5]. When the gases are energized at high energy, physical and chemical reactions with the gas release electrons, ultra-violet photons, charged particles, reactive oxidative species and ozone [2]. Large electromagnetic field is required to produce plasma at relatively low temperatures (< 104 ^{o}F) [2].

There are several types of electrical circuit which can be used to generate high voltage up to kV range [7-10]. One of the earliest circuits is Marx generator which was created by Erwin Otto Marx in 1924. It generates a high-voltage pulse using a low-voltage DC supply. The principle behind this design is by charging a number of capacitors in parallel and discharge them in series. Since a DC voltage is a constant voltage echo in the same wavelength, this charges the capacitors to the maximum potential and this discharges the stored energy in parallel. Another classical

Advances in Electrical and Electronic Engineering: From Theory to Applications
AIP Conf. Proc. 1883, 020023-1–020023-6; doi: 10.1063/1.5002041
Published by AIP Publishing. 978-0-7354-1563-8/$30.00

high voltage generator is a half-bridge voltage resonant inverter developed by Baxandall using basic *LCR* circuit connected to a midpoint [11]. The mid-point is connected via Tesla coil supplying power to a load of *LR* series circuit in parallel. This circuit also has a self-resonant frequency circuit driving the square waveform resulting in sinusoidal current flowing through a Tesla Coil. This yields with of low loss-resistance and consequently high quality factor [11]. Non-linear controlled high frequency inverter was also used to induce plasma [12]. The parallel resonant inverter consists of MOSFET switches connected to a output parasitic capacitor and a transformer to power the plasma reactor [12]. With similar switching concept, inverter based plasma source was built based on the ZVS driver flyback transformer and Tesla resonator to energize dielectric barrier discharged plasma [11]. In this circuit, a phase lock loop (PLL) oscillator generates clock signal in square wave transistor-transistor logic (TTL) signal having twice of the output signal. A pulse width modulation circuit functions as the wave generator to control the pulse switching time of the transistors.

This paper describes generation of APPJ from a low DC voltage source at 3A current rating using similar resonant inverter or zero voltage crossing switching circuit (ZVS) developed by Vladimiro Mazzilli. Mazzilli's ZVS is a derivative of the L-C MOS oscillator or Royer Oscillator [13] and it is well known for its simplicity to generate voltage ranging from 20 – 40 kV. In this work, the circuit was used with slight modification of the components. Mazilli ZVS driver is a self-resonant, push-pull, free running oscillator that uses a transformer to generate high voltage. The output of the proposed ZVS circuit was matched to a flyback transformer for further stepping up to high voltage. The alternating pulses generated enough potential to energies a plasma torch through a pair of electrodes to emit APPJ while purging with argon gas. The interaction of the APPJ plasma emission with a leaf was studied in this work.

METHODOLOGY

Falstad Simulation Setup

The Mazzilli's ZVS flyback driver as shown in Fig. 1 consists of two parts. The first part is a switching circuit with a pair of MOSFETs (IRFP260) and zener diode that step up the input 12 Vdc, 3A into high frequency sinousoidal signals which drives a flyback transformer. The switching voltage which turns on and off the MOSFET drops at a 0.66 uF capacitor rated at 1200 Vdc and 200 µH inductor that are parallel to the primary winding coil of the flyback transformer. The circuit was simulated using a Falstad software before actual configuration of the circuit in hardware.

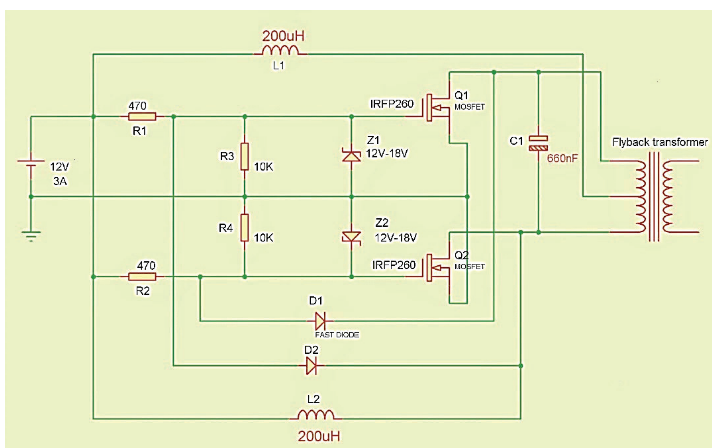

FIGURE 1. The Zero Voltage Switching (ZVS) flyback driver

Upon application of power, current flows through both sides of the MOSFET's drains. One of the MOSFETs turns on faster than the other and more current draws to this MOSFET. This causes the other MOSFET to be turn off. The voltage starts to rise and fall sinusoidally. When Q1 turns on, the voltage at drain of Q1 will be ground while voltage at source of Q2 rises to a peak and drops back down during the one half cycle of LC tank. As voltage of the source of Q2 drops to zero, the gate current to Q1 is also removed and as a result, Q1 turns off. This causes the drain voltage of Q1 to rise and Q2 turns on. The MOSFETs switch when there is least power induced. The same process repeats for the second half cycle. To prevent the oscillator from drawing huge peak currents and explodes, L1 is placed in series with the power supply functioning as a choke to mitigate current spikes. R1 limits the current that charges the gates to avoid damage of over current at the MOSFET. R3 of 10kΩ pulls the voltage down to ground to avoid latchup. The Zener diodes regulates the voltage at 18 V. D1 and D2 ensures the gates voltage down to ground when the voltage on the opposite leg of the tanks is at ground.

Circuit prototype and measurement

The red wire (+) of the secondary coil of the flyback transformer with a potential of 24.5 kV was connected to the anode of the quartz tube. The anode is a copper rod (gauge size =22) inserted into the inlet of the argon gas hose purged at a flow rate of 50 l/min (Fig. 2). The ground connection of the flyback transformer connects to the ground plate with a fixed distance from the terminal end of the plasma torch.

The waveforms were measured at each test points of the ZVS circuit at the 470 Ω resistor, IRFP260 transistors, and 0.66 µF capacitor. This circuit must be tested carefully because the transient voltage is very high and could easily damage the probe. The signal generated at high voltage was measured using an oscilloscope. The probe used was a high voltage oscilloscope probe which can measure 1000V at 1:1 rating.

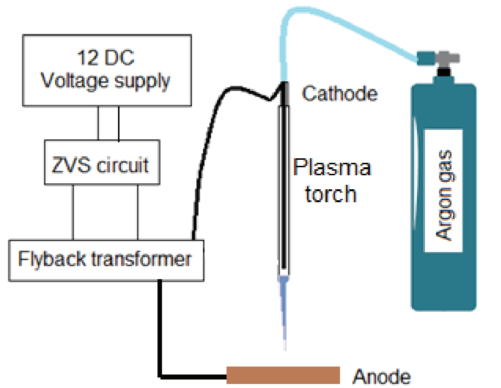

FIGURE 2. A cold atmospheric plasma device

RESULTS AND DISCUSSION

The simulated signal output of the circuit was determined using software oscilloscope feature available in the Falstad software. Figure 3 shows the DC pulses generated at the resistor of 470 Ω. After the 12Vdc 3A power supply was switched on to power the ZVS circuit, a DC ½ phase was observed at the pair of resistors. The peak voltage of the half DC pulses dropped slightly to 11.46 V as a result of the zener diode regulation.

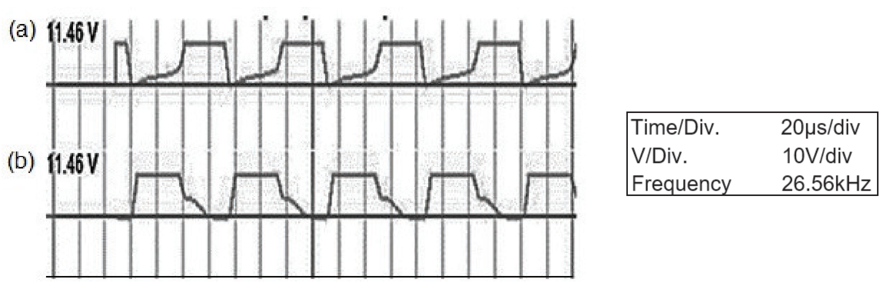

FIGURE 3. Output waveforms at the 470 Ω resistors of (a) R1 and (b) R2.

Half cycle sinusoidal signals alternatively oscillates at the drain-source (Vds) of the pair of IRFP260 MOSFET as shown in Fig. 4. The transistor is also an amplifier in the ZVS circuit for ensuring maximum power delivering to the next stage. Hence, fast switching transistor used was used. Each of the transistor connects to the inductor coil is mirrored to each other. A summary of the voltage determined at the various components in the circuit are as shown in Table 1.

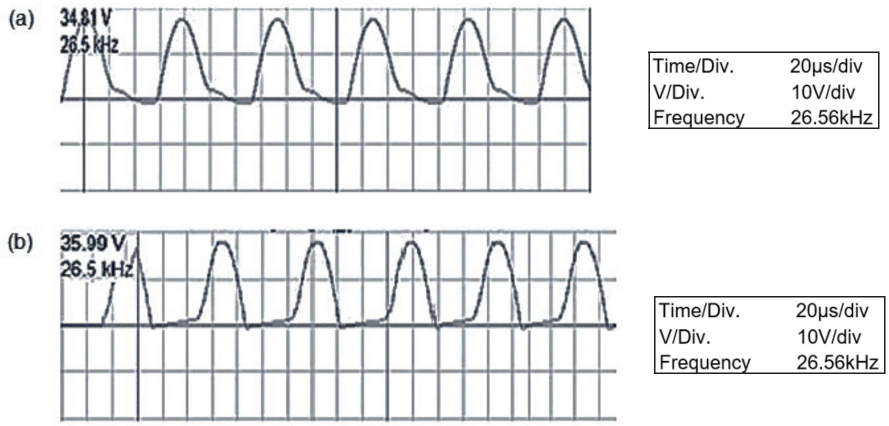

FIGURE 4. The Vds waveforms at the MOSFETS of (a) Q1 and (b) Q2.

TABLE 1. Voltage Rating of the ZVS Components

Component	Voltage (V)
Source input voltage in DC	12
Inductors	13.7
Capacitors	33.73
Vds of IRFP 260 MOSFET	35.9

The simulation result was confirmed with the measurements using an oscilloscope as shown in Fig. 5. The measurement result as shown in Fig. 5 indicates that the frequency of the MOSFET is at 50 kHz using a 12Vdc, 3A power supply as input voltage. The input voltage is variable between 10-30Vdc. During linear operation mode, the voltage increases from 0 to maximum of 35.7V and drops down as the transistor switches from ON to OFF mode. Ideally, the second cycle of the pulse starts to oscillate when the first cycle of pulse reaches zero voltage or both pulses of the two transistors crossed over at zero voltage point. However, the crossed over occurred at 7.19 V before the first cycle of pulse turned to zero voltage is as shown in Fig. 5. Voltage losses occur during hard switching of the MOSFET switches. The area under the crossed over point in the waveform as shown in Fig. 5 indicates the loss of power. These losses is proportional to the switching frequency and limits the maximum frequency operation. Although the switching loss seemed to be a problem, it happens in a fraction of second which makes the loss negligible. The losses can be reduced if the roll-off of the pulse or the rate of change of voltage (dv/dt) is increased. Another problem with hard switching is the generation of electromagnetic interference due to large change in current over a short time and hence, creating noise.

The transistors functions alternatively to charge voltage to the capacitor with the complete sinewave half-cycle of signals (Fig. 5). The switching works continuously through the ZVS driver charging the capacitor and the waveforms simulated at the capacitor is as shown in Fig. 6. However, the software failed to simulate the two cycles of half-waves charged to the capacitor as measured practically in Fig. 5. The waveforms show that the capacitor is charged through sinusoidal pulses. Each time the capacitor discharges, the voltage transfers to the flyback transformer. This process repeated continuously to ensure a constant voltage is seeded to the flyback transformer for it to work continuously until the ZVS driver is turned off. The output capacitance must be discharged and charged every cycle. At a frequency of 50 kHz for two half cycles, the calculation for power loss from the capacitor is [14]:

$$P = \frac{1}{2}CV^2 f = \frac{1}{2}600nF \cdot 36V^2 \cdot 50kHz = 19.4Watts \quad (1)$$

where P is power dissipated, C is capacitance, and V is peak voltage, thus 19.44 watts were dissipated simply from hard-switching the output capacitance. The parasitic inductance could also contributes to the power loss.

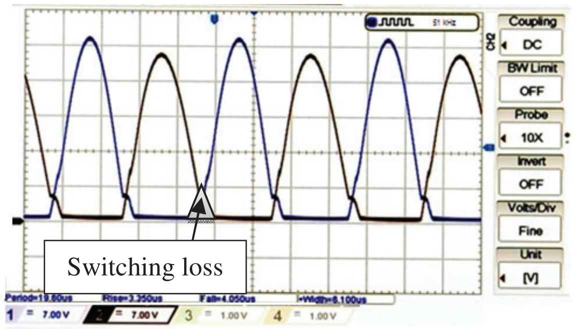

FIGURE 5. Superimposed waveforms Vds at Q1 and Q2 MOSFETS.

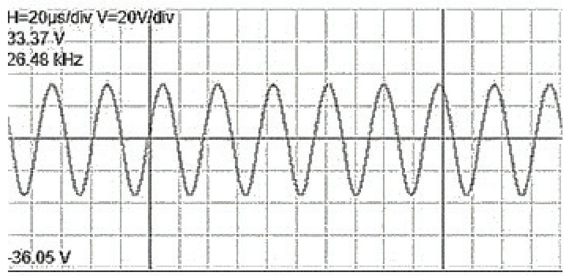

FIGURE 6. The waveform simulated at the capacitor

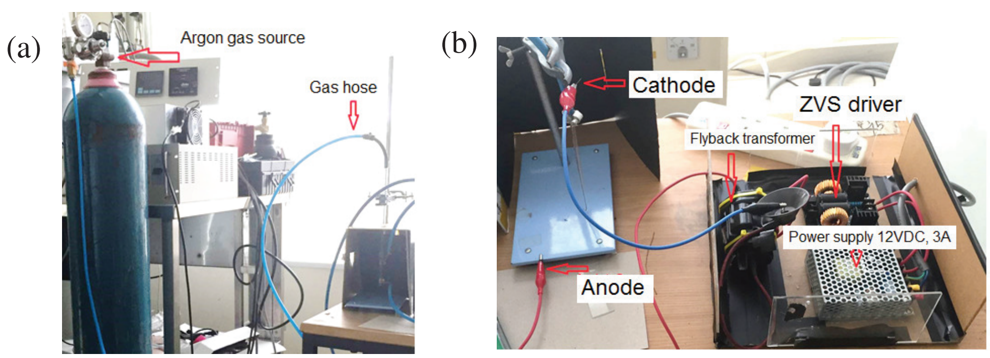

FIGURE 7. Cold atmospheric plasma system with (a) argon gas connection and (b) ZVS circuit and flyback transformer setup.

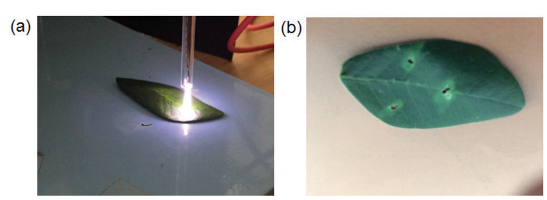

FIGURE. 8. (a) Exposure of plasma to a leaf and (b) the pin hole on a leaf after exposure to plasma jet.

A fully connected circuit with the quartz tube and argon gas supply are as shown in Fig. 7. After several adjustment on the distance between the anode and cathode, the experiment determined that the copper rod needed to be inside the quartz tube and at a distance of 1.2 cm from the base cathode to generate APPJ. The plasma produced at linear emission is as shown in Fig. 7.

The effects of the plasma exposure to a leaf for 5 seconds indicated that the plasma delivered heat which is high enough to cause burn to the leaves. Pin holes were identified after removal of the plasma jet (Fig. 8). The pin hole was not found if the plasma exposure distance was reduced to 0.2 cm from the sample. It seemed that the atmospheric plasma generated is destructive and generated heat which caused burn to the leaf at a longer distance of 1.2 cm. This could be related to the high power produced from circuit. A similar APPJ system using a power booster with 400 kV, 1 kHz DC pulses [3] developed by our group was applied to a leaf but it was found not causing burning effect to the leaf. This could probably associated with the lower frequency used. However, the result is not reported here and it is subjected to further investigation to compare both system.

CONCLUSION

A ZVS driver with flyback transformer was successfully used to generate cold atmospheric plasma in a lower voltage source setup. The operation of the circuit was simulated with flastad software and the output waveforms were verified through circuit measurements. The advantage of the circuit proposed is the use of low DC pulsed voltage supply (12V, 3A) which was stepped up to high voltage (24.5 kV) with relative losses at 19.4 watts and provided sufficient energy to the plasma torch for generation of plasma using argon gas. The output of the plasma generated was found destructive which caused pin holes on a leaf after exposure to plasma jet.

ACKNOWLEDGMENT

The authors are grateful to the Short Term Grant (STG) Vot No. U641 awarded by Universiti Tun Hussein Onn Malaysia.

REFERENCES

1. A. Schutze, J. Y. Jeong, S. E. Babayan, J. Park, G. S. Selwyn and R. F. Hicks. IEEE Transactions on Plasma Science. **26**, 1685-1694 (1998).
2. M. N. Firdaus Zainal, N. Redzuan and M. F. Ikmal Misnal. Jurnal Teknologi. **74**, 57-61 (2015).
3. E. Rizan Rizon, M. K. Ahmad, N. Nafarizal, M. Z. Sahdan and C. F. Soon. in *IEEE-ICSE 2016 Prococeedings* (IEEE, Kuala Lumpur, 2016).
4. C. Hoffman, C. Berganza and J. Zhang, Medical Gas Research. **3**, 1-21 (2013).
5. M. Keidar, A. Shashurin, O. Volotskova, M. A. Stepp, P. Srinivasan. A. Sandler and B. Trink, Physics of Plasma. **20**, 1-8 (2013).
6. M. Nagatsu, M. Kinpara and T. Abuzairi, in *Recent Global Research and Education: Technological Challenges, Advances in Intelligent Systems and Computing* edited by R. J. a. R. S. (eds.) (Springer International Publishing, Poland, 2017), Vol. 519.
7. D. Y. Lee, D. S. Hyum and I. Choy, IEEE Transactions on Plasma Science (2002).
8. B. Liu, S. Duan and X. Li, Preglad Eletroechniczny (Electrical Review). **88**, 278-282 (2012).
9. H. Fujita and H. Akagi, IEEE Transactions on Industry Applications. **35**, 21-28 (1999).
10. Y.-N. C. and C.-M. K., Journal of Applied Research and Technology. **11**, 225-234 (2013).
11. S. D. Anghel, IEEE Transactions on Plasma Science. **39**, 871-876 (2011).
12. S. Zerouali, A. Hadri-Hamida and M. Belloufi, International Journal of Advanced Science and Technology. **69**, 33-46 (2014).
13. D. Edry and S. Ben-Yaakov, . IEEE Transactions on Aerospace and Electronic Systems. **29**, 1287-1296 (1993).
14. S. L. McClusky, Master Thesis, California Polytechnic State University, 2010.